Appendix: MRI Acquisition, Image Analysis and Quantification Variability

Circulation Revision – 2008 07-29

Delayed Enhancement MRI Acquisition – Detailed Parameters

Patients who were referred to the University of Utah for pulmonary vein antrum isolation (PVAI) were included in this analysis. In all patients, a contrast enhanced 3D FLASH angiography sequence and a cine true-FISP sequence were used to define the anatomy of the left atrium (LA) and the pulmonary veins (PV). To depict fibrous regions of the left atrium, delayed enhancement MRI was acquired approximately 15 minutes after contrast agent injection using a 3D inversion recovery prepared, respiration navigated, ECG gated, gradient echo pulse sequence. The sequence was based upon previously reported work.[1, 2] Typical acquisition parameters were: free-breathing using a respiratory navigator with a 6 mm acceptance window, a transverse imaging volume with voxel size = 1.25 x 1.25 x 2.5 mm (which was then reconstructed to 0.625 x 0.625 x 1.25 for analysis), TR/TE = 6.3/2.3 ms, TI = 230-270 ms, flip angle = 22°, bandwidth = 220 Hz/pixel, 1 RR interval between inversion pulses, phase encoding in right-left direction, parallel imaging using the GRAPPA technique with R = 2 and 32 reference lines, partial Fourier acquisition with 0.875 factors in the phase-encoding direction and a 0.8 factor in the slice-encoding direction.

ECG gating was used to acquire a small subset of phase encoding views and during the diastolic phase of the left atrial cardiac cycle. The time interval between the R-peak of the ECG and the start of the data acquisition was defined by examining the cine images of the left atrium to determine the period of minimal left atrial motion. The typical value of the interval was 60% of the mean RR interval for patients in sinus rhythm and 50% of the mean RR for patients with non-regular heart rate. The respiratory navigator was used to acquire data during the end of the expiration phase the respiratory cycle. To reduce the negative effect of respiration of image quality and resolution, the navigator was positioned on the right hemi-diaphragm. The acceptance window was set to ± 3 mm. The typical LA motion due to respiration is predominantly in the superior/inferior (S/I) direction. This motion has lower amplitude than the corresponding diaphragm motion. From our observations, we have noted that the typical LA motion amplitude in the S/I direction is about two times smaller

than the diaphragm S/I displacement. Thus, the data acquisition for the delayed enhancement pulse sequence was active only if the LA displacement was less than 1.5 mm from the baseline. The voxel size (spatial resolution) of our pulse sequence in the S/I direction 2.5 mm. Therefore, data was only acquired if the LA displacement in the S/I direction was less than half of the voxel size in the same direction.

To resolve the effect of the left atrial motion due to cardiac activity on image quality and resolution, data was acquired only during the diastolic phase of the LA. Cine images of the LA were used to identify the time interval when the LA motion was minimal. The parameters of the delayed enhancement pulse sequence were adjusted so that the data acquisition occurred during this time interval. It was further restricted to approximately 120 ms per heartbeat.

Fat saturation was used to suppress the fat signal. The TE of the scan was chosen such that the signal intensity of partial volume fat-tissue voxels was reduced allowing improved definition of the left atrial wall boundary. The TI value for the DE-MRI scan was identified using a scout scan. The typical scan time for the DE-MRI study was between 5 to 9 minutes depending on the subject respiration and heart rate.

Many of the early patient scans included some high signal artifact induced by the respiratory navigator positioned on the right hemi-diaphragm. Figure A1 shows an example of such a scan where it is possible to see navigator induced bright blood signal in right pulmonary veins, the most common location of the artifact. However, despite the presence of navigator artifact, there is a strong qualitative relationship between the color MRI model (Figure A1c) and the electroanatomic map acquired during the catheter study (Figure A1d). To remove the artifact complementary re-inversion RF pulse was removed from the product implementation of the navigation scheme and navigation information was acquired following imaging data. The change preserves the inversion recovery magnetization preparation in the whole image volume and results in a more uniform blood signal in the pulmonary vein and left atrium. Figure A2 shows an example of a later scan without the navigator artifact.

Analysis of Delayed Enhancement-MRI Images

The threshold for fibrosis identification was determined for each patient individually by using a dynamic threshold algorithm based partly on work in the left ventricle.[3, 4] Figure A3 provides an overview of the data processing steps of the algorithm. First, slices from the DE-MRI scan are windowed and cropped. The epicardial and endocardial borders are then manually traced to isolate the walls of the left atrium. The algorithm then automatically selects a threshold intensity which is likely to correspond to the enhanced/fibrotic voxels of the left atrium by estimating the mean value and the standard deviation of the "normal" tissue. "Normal" tissue is defined as the lower region of the pixel intensity histogram between 2% and 40% of the maximum intensity within the region of interest (e.g., the left atrial wall). The enhanced/fibrotic threshold was then calculated as two to four standard deviations above the mean of "normal." These values cover from 95% to 99.994% of a Gaussian distribution. The threshold was determined on a slice by slice basis and the region identified as fibrotic was then compared to the original DE-MRI slice for appropriateness. The most commonly used cutoff was three standard deviations.

The overall volume of the LA myocardium was calculated as the number of voxels within the endocardial and epicardial contours. The extent of enhancement was then calculated as the number of pixels identified as enhanced by the semi-automated algorithm over the volume of the left atrial myocardium for the slice.

Inter and Intra-Observer Agreement

Inter-observer Agreement

For interobserver agreement, observers 1 and 2 both analyzed a subset of 43 patients from the clinical cohort with high quality DE-MRI scans. The two observers were blinded to the results obtained by the other observer and analyzed the studies by following a set protocol. First, the endocardial contour was traced and care was taken to avoid the pulmonary veins. Second, the epicardial contour was traced. The data was then quantified using the semi-automated algorithm by a third individual according to the described methodology.

The limits of agreement were calculated by Bland-Altman analysis. The difference between the amount of enhancement detected from the segmentation of observer 1 and observer 2 was taken and plotted against the average detected enhancement from the segmentations of observers one and two. The average difference and 95% confidence interval (limits of agreement [LOA]) were calculated from these plots. Figure A4 shows the Bland-Altman plot for the inter-observer agreement of detected LA wall enhancement in forty-three patients. The average difference was -0.9% (LOA = -7.9% to 6.1%).

Intra-observer Agreement

The intra-observer agreement was calculated from a set of 10 patients which were segmented two times by the same observer. The average difference and LOA were calculated in a manner similar to that described for the inter-observer agreement. The difference between segmentation 1 and segmentation 2 from the same observer was determined and plotted against the average detected enhancement. Figure A5 shows the Bland-Altman plot for the intra-observer agreement of detected LA wall enhancement in the ten patients. The average difference was 0.49% (LOA = -4.96% to 5.95%).

Relationship between EA Maps and MRI Volume Models

Qualitative Assessment

A trained expert qualitatively assessed and graded the relationship between EA maps and MRI color models. The relationship was rated on a 0 to 4 scale where 0 was coded as “No Relationship,” 1 was coded as “Poor”, 2 was graded as “Mediocre”, 3 as “Good”, and 4 as “Excellent”. The average relationship between EA maps and MRI models was 3.65 ± 0.55 (range 2 to 4). Figure A6 shows an example of a strong qualitative MRI correlation with the corresponding EA map. The region of low voltage tissue has been highlighted in white on the electroanatomic map.

Quantitative Assessment

Fifty-four patients with high quality CartoXP maps (defined as greater than 100 voltage points evenly spread throughout the atrium) were selected and scored by blinded reviewers. The same was done using three

dimensionally rendered DE-MRI models. The LA was then subdivided into 18 specific regions (9 on the posterior wall) and 9 on the anterior and septal wall. Figure A6 shows the posterior wall projections of a DE-MRI volume model and electroanatomic map for the same patient. In both images, the 9 box grid used for scoring has been applied.

Four blinded reviewers (two individuals experienced in cardiac MRI and two individuals experienced in atrial fibrillation ablation) separately scored the MRI models and electroanatomic maps. Two views of interest, the posterior (PA) and right anterior oblique which shows the anterior wall and septum [RAO]), were chosen for scoring.

The images were scored on a 0 to 3 scale. For MRI models, 0 was scored as no enhancement, 1 as mild enhancement, 2 as moderate, and 3 as extensive enhancement. For EA maps, 0 was considered healthy tissue (voltage > 1 mV, purple on EA maps), 1 was considered as mild illness (some abnormal tissue where voltage was > 0.1 mV and < 0.5 mV), 2 as moderate illness (presence of low voltage tissue [voltage > 0.1 mV and < 0.5 mV] as well as fibrotic scar [voltage < 0.1 mV]), and 3 as scar (voltage < 0.1 mV, red on EA maps). The overall score was a sum of all nine regions for both the posterior wall and the septum. The reviewer scores were then averaged to determine the score used in quantitative analysis. The relationship between EA maps and MRI was then analyzed using pairwise regression.

Figure A8 shows the analysis between the extent of enhancement on MRI and the amount of low voltage tissue. A positive correlation of $R^2 = 0.61$ was noted.

References

1. McGann C, Kholmovski EG, Oakes RS, et al. Magnetic Resonance Imaging Detects Chronic Left Atrial Wall Injury Post Ablation of Atrial Fibrillation. Paper presented at: Scientific Sessions - AHA 2007, 2007; Orlando, Florida.

2. Peters DC, Wylie JV, Hauser TH, et al. Detection of pulmonary vein and left atrial scar after catheter ablation with three-dimensional navigator-gated delayed enhancement MR imaging: initial experience. *Radiology.* Jun 1 2007;243(3):690-695.

3. Hsu LY, Natanzon A, Kellman P, Hirsch GA, Aletras AH, Arai AE. Quantitative myocardial infarction on delayed enhancement MRI. Part I: Animal validation of an automated feature analysis and combined thresholding infarct sizing algorithm. *J Magn Reson Imaging.* Mar 2006;23(3):298-308.

4. Hsu LY, Ingkanisorn WP, Kellman P, Aletras AH, Arai AE. Quantitative myocardial infarction on delayed enhancement MRI. Part II: Clinical application of an automated feature analysis and combined thresholding infarct sizing algorithm. *J Magn Reson Imaging.* Mar 2006;23(3):309-314.

Appendix – Figure A1. Example of early DE-MRI acquisition showing a substantial artifact induced by the respiratory navigator placed on the right hemidiaphragm. (A) 2D MRI slice from DE-MRI scan. **(B)** Maximum intensity projection (MIP) of segmented 2D slices. **(C)** MRI images as volume rendered three dimensional model. **(D)** Electroanatomic map acquired during invasive EP study. When present, the artifact was primarily localized to the right pulmonary veins and varied substantially in intensity. Despite the presence of an artifact, there is still a relationship between the color MRI (C) and the electroanatomic map (D). The patient shown has minimal enhancement.

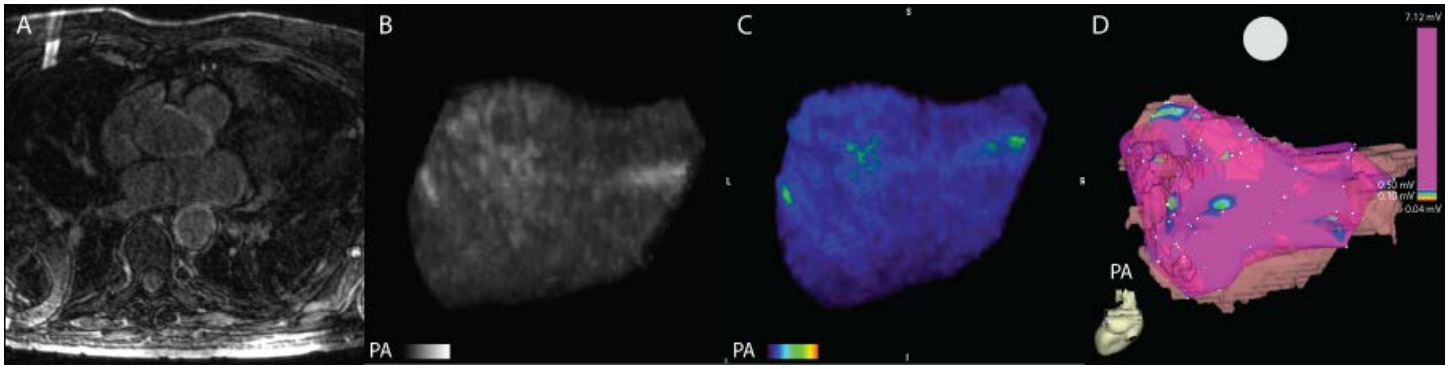

Appendix – Figure A2. Example of DE-MRI without navigator induced artifact. 2D MRI slice from DE-MRI scan. In contrast to the image shown in Figure A2, there is no visible navigator artifact on the right side. The patient shown has minimal enhancement.

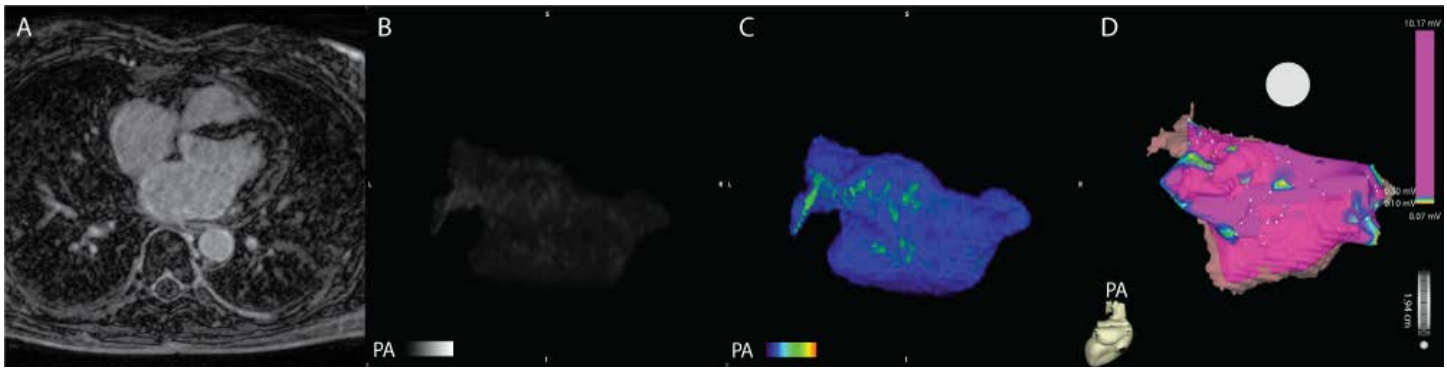

Appendix – Figure A3. Data flow of the semi-automated algorithm used for detection of abnormal enhancement. The input slices from the delayed enhanced scan were windowed and cropped. The epicardial and endocardial borders were then manually segmented. The algorithm then automatically selected a threshold intensity which was likely to correspond to the enhanced/fibrotic voxels of the LA by estimating the mean value and standard deviation of the lower region of the pixel intensity histogram. The threshold cutoff was chosen manually at two to four standard deviations above the mean for the lower histogram region and assessed by an observer for appropriateness. If the algorithm has over estimated or underestimated the degree of enhancement, the cutoff was adjusted appropriately.

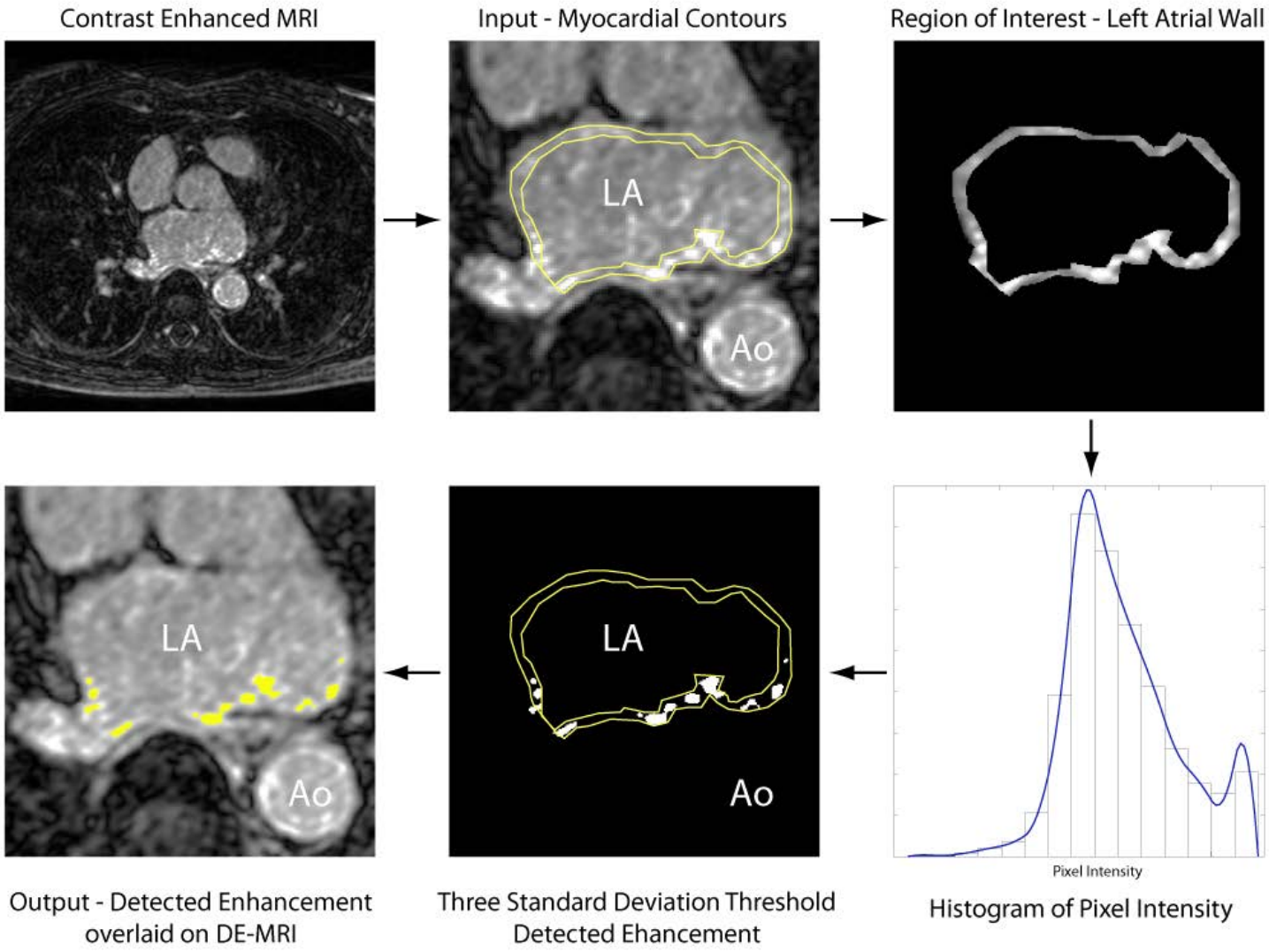

Appendix – Figure A4. Bland-Altman plot for the inter-observer agreement of detected LA wall enhancement in 43 patients. The quantified inter-observer values were taken from the analysis of two reviewers (Reviewer 1 and Reviewer 2).

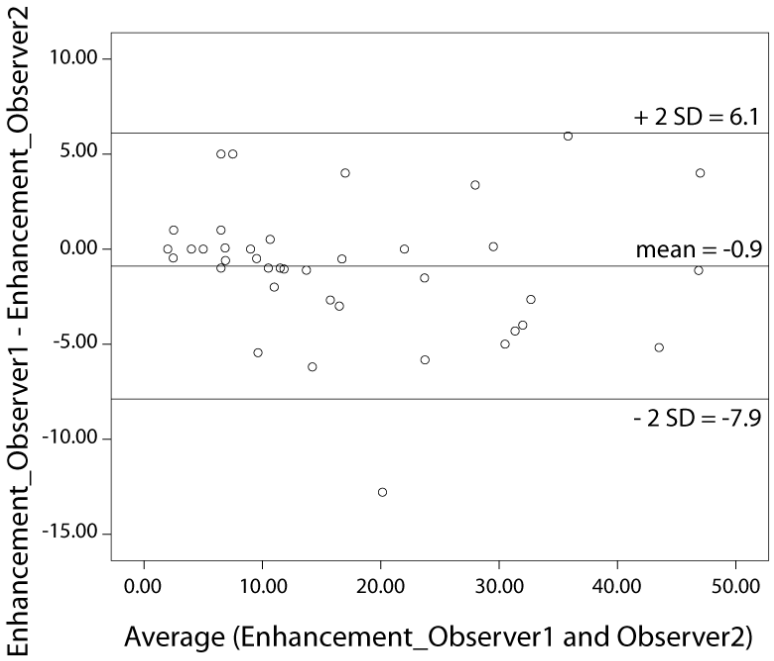

Appendix – Figure A5. Bland-Altman plot for the intra-observer variability of fibrosis detection (left) and LA volume segmentation (right) in ten patients. The quantified intra-observer values were taken from separate analyses performed by the same reviewer (Reviewer 1).

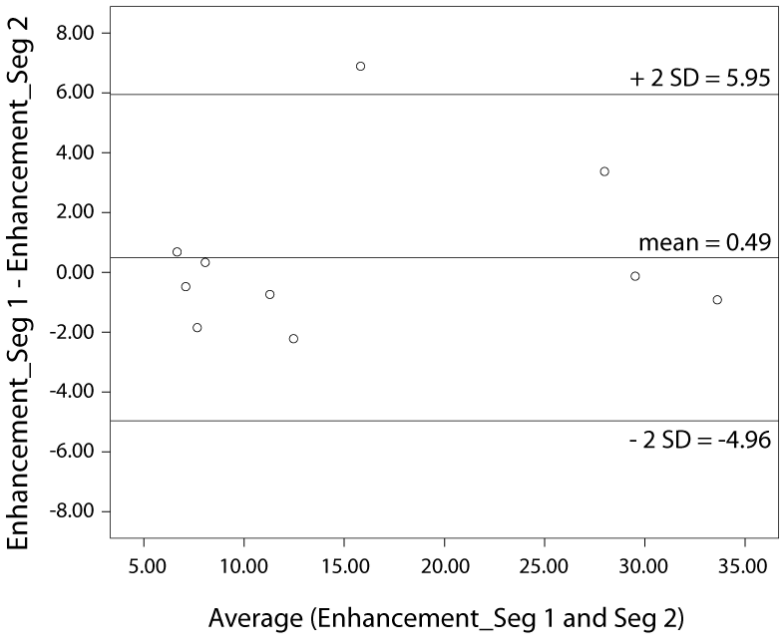

Appendix – Figure A6. Example of a strong qualitative MRI correlation with EA map, posterior (PA) view.

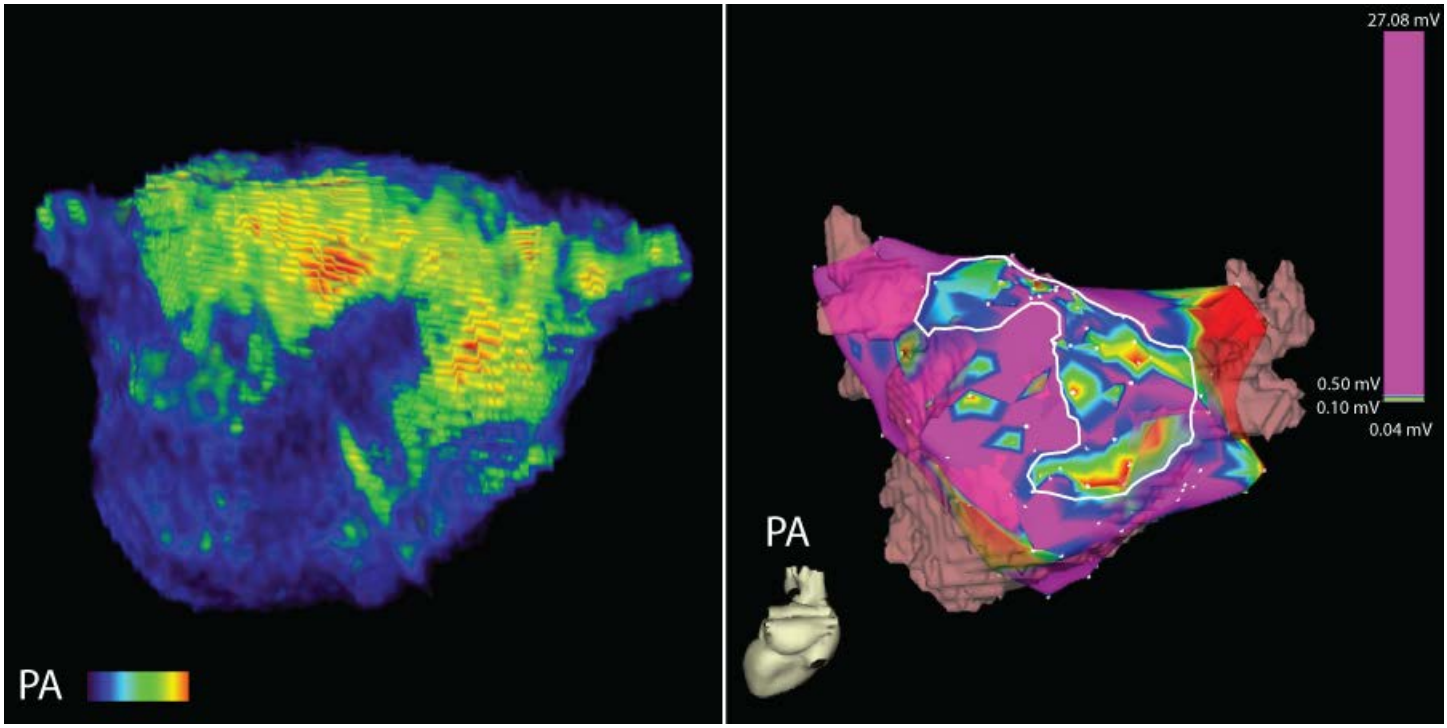

Appendix – Figure A7. Posterior wall projections of DE-MRI volume model (left) and electroanatomic (EA) map acquired with the CARTO system (right). In both images, the a 9 box grid was used for qualitative scoring. 18 separate regions covering the posterior wall and, the interatrial septum, and the anterior wall were evaluated. Both the DE-MRI models and the EA maps were scored from 0 (no abnormal enhancement/disease) to 3 (severe enhancement/disease). The overall score was a sum of all nine regions for both the posterior wall and the septum.

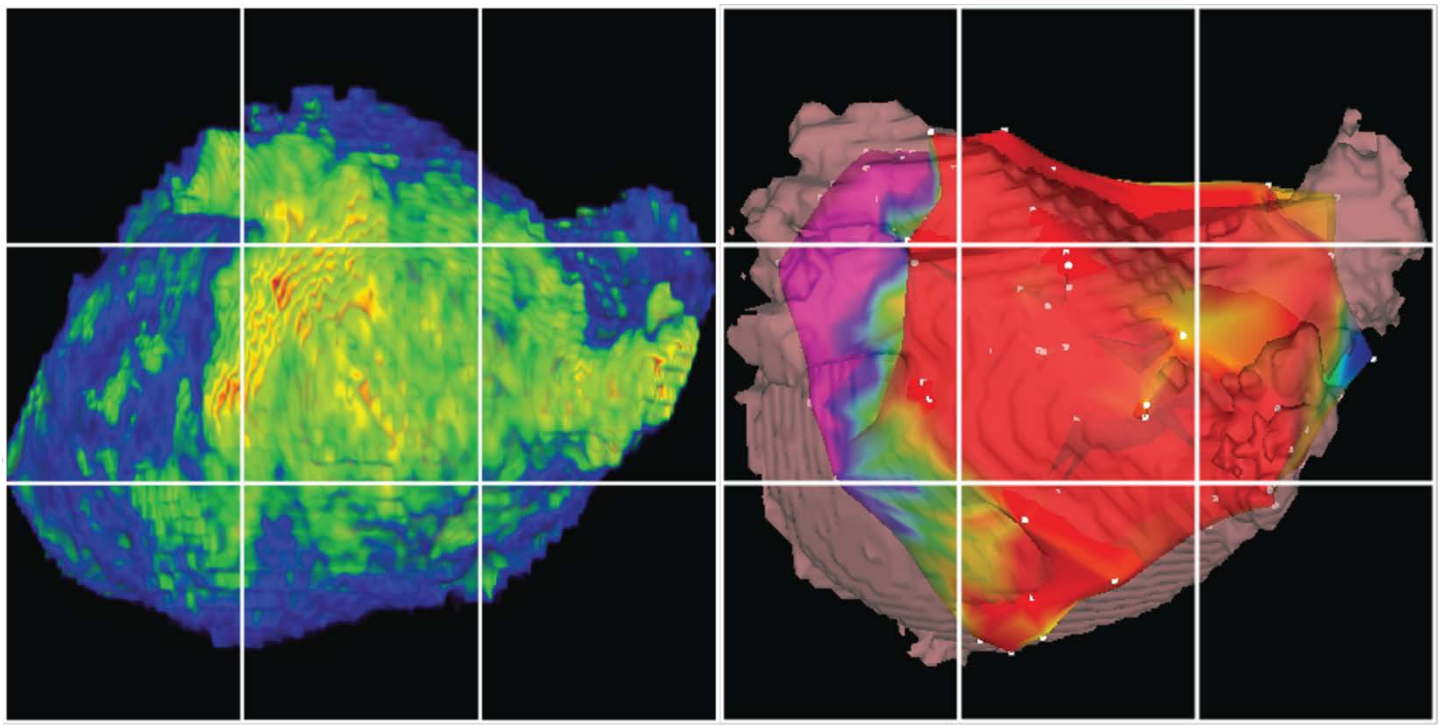

Appendix – Figure A8. Pairwise regression between the extent of enhancement (MRI) and the amount of low voltage tissue (graded by blinded reviewers).